Comparative Analysis of Temperature Control Strategies: Open-Loop, On-Off, and PID-Based Regulation

Joonwoo Noh(260973555), Keonwoo Kim(260914383)

McGill University Department of Physics

March 17, 2025

Abstract

We implemented five different control methods—open-loop, on/off, proportional, proportional-integral, and proportional-integral-derivative—to regulate the power system and ensure the aluminum rod reaches the setpoint of 100°C with maximum precision. Open-loop tests revealed heating and cooling time constants of 674.71 ± 0.01 s and 718.69 ± 0.01 s, respectively, while on/off control demonstrated straightforward operation but led to temperature oscillations that varied with hysteresis. A fully tuned PID controller minimized overshoot and improved settling times relative to simpler methods. Furthermore, based on the measured data, we calculated the heat capacity of aluminum to be 35 ± 1 J/K.

Contents

1 Introduction **1**

2 Materials and Methods **2**

3 Part 1: Open-Loop Operation **3**

3.1 Results 3

3.2 Discussion 3

4 Part 2: On-Off Control **4**

4.1 Results 4

4.2 Discussion 5

5 Part 3: Proportional Control **5**

5.1 Results 5

5.2 Discussion 6

6 Part 4: Proportional-Integral Control **6**

6.1 Results 6

6.2 Discussion 7

7 Part 5: Proportional-Integral-Derivative Control **8**

7.1 Results 8

7.2 Discussion 9

8 Part 6: Heat Capacity **9**

9 Conclusions **10**

1 Introduction

Temperature control is a fundamental requirement in various fields. Effective temperature regulation is essential for system stability and process efficiency. In this experiment, a servo-based temperature control system regulates the temperature of an aluminum block. The system continuously monitors the block's temperature, compares it to a desired setpoint, and dynamically adjusts heater power using pulse-width modulation (PWM). The effectiveness of temperature control is evaluated using three different control strategies:

1. On-Off Control: The heater is fully activated when the temperature is below the setpoint and completely deactivated when it exceeds the setpoint. This leads to oscillations around the desired temperature due to continuous switching.

2. Proportional (P) Control: The power supplied to the heater is proportional to the difference between the setpoint temperature T_s and the measured temperature T_m:

$$P = (0.5 + E) \times P_{\max} \tag{1}$$

where the error E is defined as:

$$E = \frac{T_s - T_m}{B} \tag{2}$$

and B is the proportional band, determining the range over which power is adjusted.

3. Proportional-Integral-Derivative (PID) Control: To improve system stability and accuracy, integral and derivative terms are added:

$$P = (0.5 + E + K_i I + K_d D) \times P_{\max} \tag{3}$$

where $I = \int E dt$ is the integral action that keeps increasing the power output until the error is eliminated as long as the error persists, $D = -\frac{dE}{dt}$ is the derivative action that reduces overshoot by responding to the rate of change of error, which means that if the temperature is rising too quickly, the derivative action reduces the control signal to slow down the increase and vice versa, and lastly, K_i and K_d are the gain factors associated with the integral action time (IAT) and derivative action time (DAT), respectively. They should be tuned based on the system's response time [1].

The goal of this experiment is to analyze the performance of different control techniques by evaluating control accuracy, stability, and response time. A well-tuned PID controller should minimize overshoot, eliminate steady-state error, and provide a fast response to temperature changes.

2 Materials and Methods

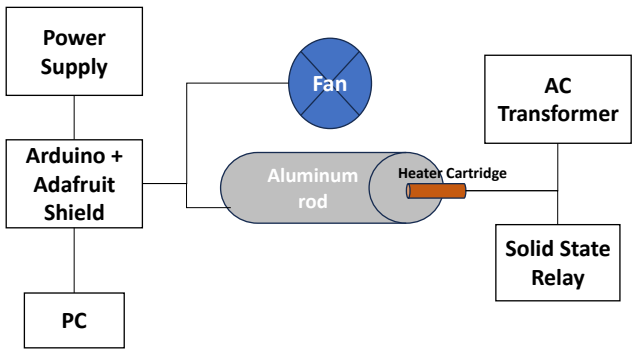

Figure 1: Schematic of the temperature control apparatus.

An aluminum block with an embedded cartridge heater and Type-K thermocouple was used as the thermal load. The thermocouple output was amplified and digitized by a MAX31856 breakout board, which interfaced an Arduino Uno. A solid-state relay (SSR)

controlled the AC power from a transformer to the heater, using a low-frequency (1 Hz) PWM signal from Arduino. Additionally, an Adafruit Motor Shield (V2) was mounted on the Arduino to drive a 12 V cooling fan. Temperature readings and control signals were sent over serial to a Python script for real-time plotting.

3 Part 1: Open-Loop Operation

3.1 Results

For this experiment, a fixed PWM duty cycle (8000) was applied to the cartridge heater while monitoring the temperature rise of the aluminum block. After reaching a quasi-steady temperature, the power was switched off to observe the natural cooling. A non-linear curve fit was applied to each temperature dataset, yielding a heating time constant of approximately $674.71 \pm 0.01s$ and a cooling time constant of approximately $718.69 \pm 0.01s$. These 0.01s uncertainties represent the inherent variability and measurement noise of the heating apparatus. Fig. (2) shows representative plots of the heating and cooling profiles, respectively.

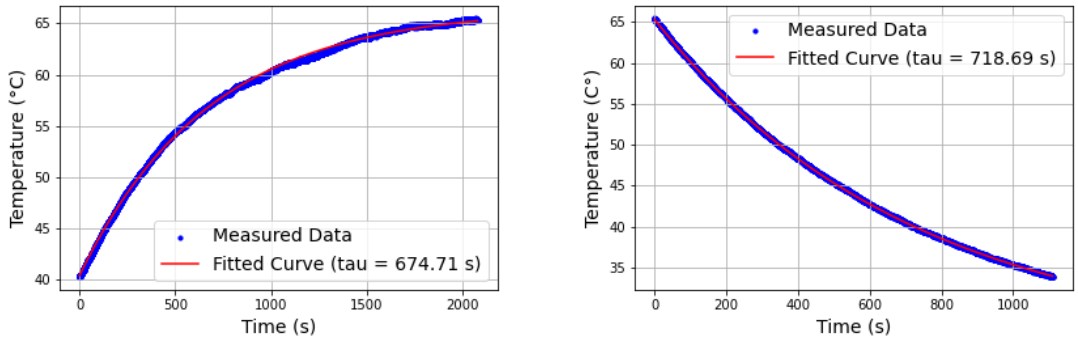

(a) (b)

Figure 2: Temperature response of the system: (a) heating under fixed PWM and (b) natural cooling.

3.2 Discussion

In open-loop mode, heater power is fixed, so ambient or load changes are uncompensated. The system settles at an equilibrium where heat input matches heat loss. Curve fits reveal heating

and cooling time constants (674.71 ± 0.01 s and 718.69 ± 0.01 s) that exceed aluminum's bulk properties alone, reflecting heat-transfer paths—conduction into supports, convective airflow, and sensor delays—that effectively enlarge the system's thermal mass.

These large time constants cause a slow response to power changes, requiring minutes to reach new equilibria. This slow response strongly affects feedback control, mandating careful tuning of integral and derivative terms to avoid wind-up or oscillation. Hence, open-loop data provide a critical baseline before moving on to closed-loop (On-Off, PID) strategies.

4 Part 2: On-Off Control

4.1 Results

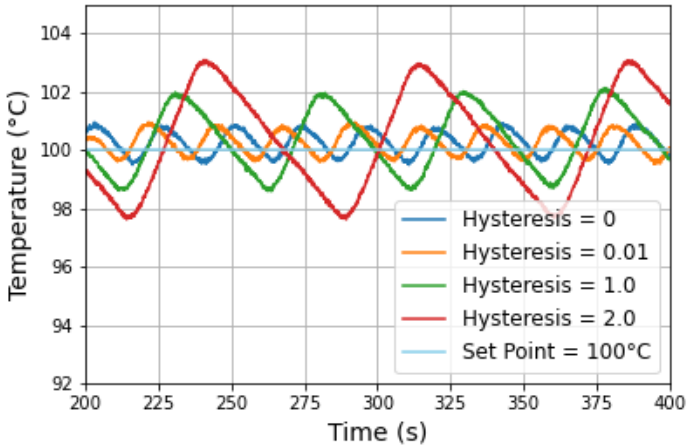

Figure 3: On-Off temperature response for different hysteresis values: 0 (blue), 0.01 (orange), 1.0 (green), and 2.0 (red). Larger hysteresis yields larger oscillations around the setpoint.

An On-Off controller was tested at a fixed PWM duty cycle (50000) with four hysteresis values: 0 (none), 0.01, 1.0, and 2.0. As shown in Fig. (3), higher hysteresis widens the temperature band around the setpoint before switching, producing larger oscillation amplitudes but less frequent toggling. Curves at 0 and 0.01 hysteresis overlapped, effectively behaving like a pure On-Off scheme. During heating, the temperature overshot the switch-off threshold by approximately 1.0°C for hysteresis 1.0 and 2.0, while on cooling it dipped below the switch-on threshold very slightly by less than 0.5°C, reflecting the difference between heating and cooling time constants and the block's thermal inertia.

4.2 Discussion

Larger hysteresis broadens the allowable temperature range, reducing rapid switching at the cost of greater temperature swings. The distinct heating and cooling time constants lead to overshoot and undershoot, contributing to a sawtooth-like profile. When hysteresis is nearly zero, it is indistinguishable from a pure On-Off setup, since 0.01 °C makes no practical difference against sensor noise and slow thermal response.

5 Part 3: Proportional Control

5.1 Results

To examine the impact of the proportional band (Pb), we tested four different values of Pb: 20, 10, 5, and 1 with the same initial temperature of 95°C. As shown in Fig. (4) and Table (1), we found that a smaller Pb generally resulted in a shorter response time—the duration needed to reach stable control— and a steady temperature closer to the target temperature of 100°C. Notably, when Pb was set to 1, the temperature exhibited oscillations around its steady-state value, whereas for the other Pb values, no significant oscillations were observed.

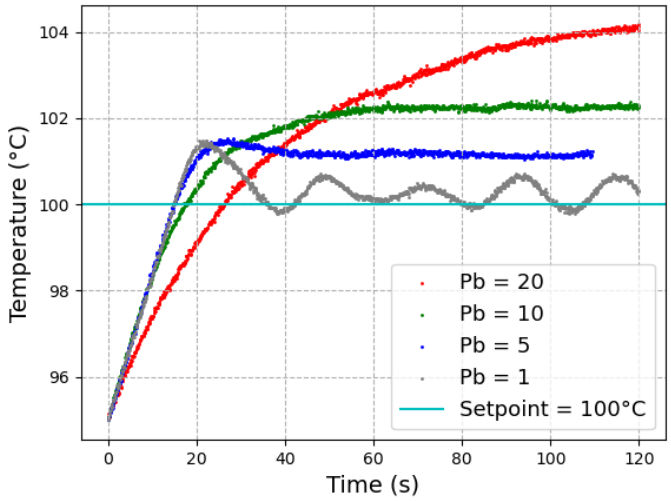

Figure 4: Temperature variations for different Pb values—20°C (red), 10°C (green), 5°C (blue), and 1°C (gray)—were examined with a setpoint of 100°C. To enhance clarity in visualization, we truncated the scattered data for Pb = 1, though all data points were included in the analysis.

Band Size	Response Time (s)	Steady State Temperatures (°C)
20	145.1 ± 0.1	104.320 ± 0.004
10	91.9 ± 0.1	102.265 ± 0.006
5	53.9 ± 0.1	101.161 ± 0.005
1	(undefined due to oscillation)	$100.16 \pm 0.01^*$

Table 1: Response times and steady state temperatures with uncertainties for different band sizes using a P control. *It's an average temperature of the oscillations.

5.2 Discussion

Reducing the proportional band can enhance the controller's accuracy, as it will require a smaller error to achieve the same change in output. Even when the system remains stable without oscillations at Pb = 20°C, 10°C, and 5°C, a slight deviation always exists between the measured temperature and the setpoint. This occurs because a proportional controller adjusts the output in direct proportion to the error but does not fully eliminate it. However, when Pb is reduced further—specifically to Pb = 1 in our experiment—temperature oscillations reappear, resembling the On-off control (4). To address this issue, we implemented integral action in the following section.

6 Part 4: Proportional-Integral Control

6.1 Results

We incorporated integral action into the proportional power control system. As illustrated in Fig. (5), when $K_i = 1$, the temperature initially overshot to approximately 104°C and then oscillated between 99°C and 102°C at a constant frequency. In contrast, for $K_i = 0.1$ and $K_i = 0.05$, after an initial overshoot near 102°C, the temperature gradually damped and settled at 100°C. For $K_i = 0.005$, the oscillation or damping behavior was not shown. It rather gradually got closer to the set point. Among the tested K_i values, $K_i = 0.1$ provided the most precise steady-state temperature at 100°C, while $K_i = 0.05$ gave the shortest response time, as shown in Table (2).

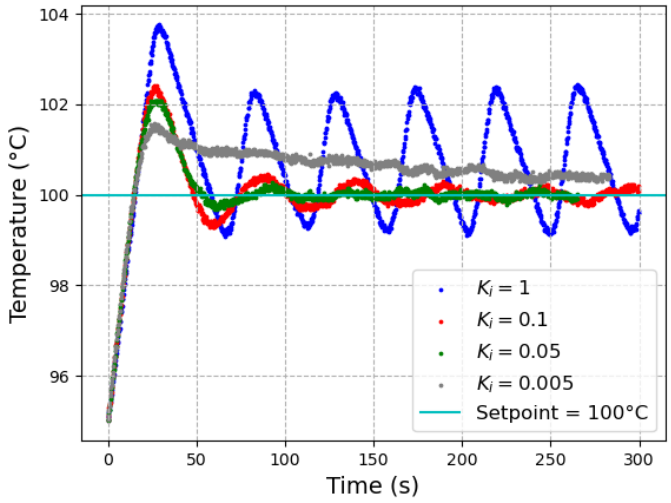

Figure 5: Temperature variations for different K_i values—1 (blue), 0.1 (red), 0.05 (green), and 0.005(gray)—were examined with a setpoint of 100°C and Pb = 5°C.

K_i	**Response Time (s)**	**Steady State Temperatures (°C)**
1	(undefined due to oscillation)	$99.43 \pm 0.02^*$
0.1	115.1 ± 0.1	99.980 ± 0.006
0.05	69.6 ± 0.1	99.933 ± 0.007
0.005	182.9 ± 0.1	100.402 ± 0.005

Table 2: Response times and steady state temperatures with uncertainties for different K_i values using a P-I control. *It's an average temperature of the oscillations.

6.2 Discussion

When $K_i = 1$, this is essentially equivalent to adding integral action to proportional control without adjusting the integral action time (IAT). As a result, the temperature oscillates and performs even worse than proportional control alone, as shown in Fig. (5). This oscillation occurs because a large K_i causes the integral term to respond too aggressively, leading to overshoot. The system then attempts to correct this overshoot, resulting in sustained oscillations. By adjusting K_i to 0.1, the IAT was properly tuned to match the system's response time, allowing the temperature to stabilize accurately near the setpoint. Furthermore, as we decrease K_i we found that the oscillation behaviors get weaker because the integral term accumulates error more slowly, leading to a less aggressive correction and improving stability

at the cost of a slightly slower response time. Thus, for $K_i = 0.005$, the smallest value we tested, oscillations are hardly noticeable, but the system takes too long to approach the set point.

7 Part 5: Proportional-Integral-Derivative Control

7.1 Results

A PID controller with a Pb of 5.0 °C was tested at two integral gains ($K_i = 0.05$ and $K_i = 1.0$), each with four derivative gains ($K_d = 0.01,\ 0.1,\ 0.5,\ 1.0$). Fig. (6) shows example temperature responses from 92 °C to a 100 °C setpoint. As summarized in Table (3), for $K_i = 0.05$ all K_d values converged within ±0.25 °C, although higher K_d slowed the final settling. At $K_i = 1.0$, persistent oscillations precluded stable convergence, even though average temperatures hovered near 100°C.

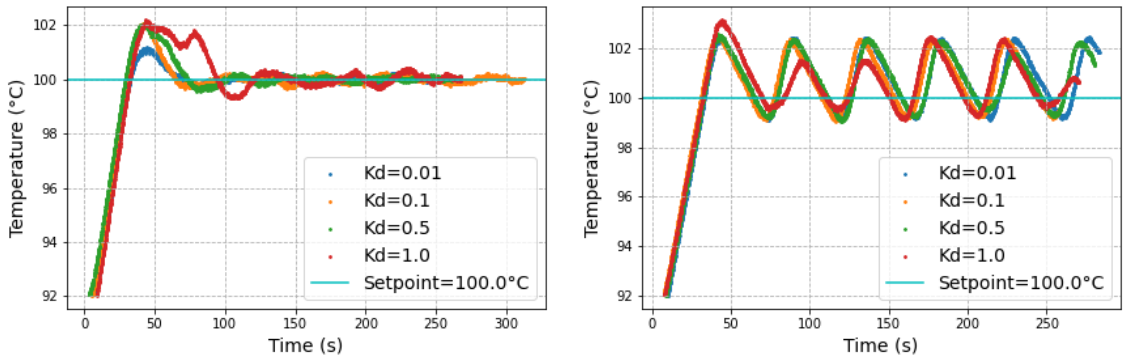

(a) (b)

Figure 6: PID temperature plots for K_i equivalent to (a) 0.05 and (b) 1.0, and various K_d. Temperature variations for different K_d values—1 (red), 0.5 (green), 0.1 (orange), and 0.01(blue)—were examined with a setpoint of 100°C, Pb = 5°C

K_d	**Response Time (s)**	**Steady Temp (°C)**
$K_i = 0.05$		
0.01	62.26	100.014 ± 0.005
0.1	83.69	99.965 ± 0.006
0.5	95.73	100.025 ± 0.005
1.0	136.62	100.022 ± 0.005
$K_i = 1.0$		
0.01	Undefined	102.07 ± 0.02
0.1	Undefined	99.30 ± 0.01
0.5	Undefined	101.68 ± 0.03
1.0	Undefined	100.745 ± 0.008

Table 3: Response time (s) and steady state temperature (°C) results at two different K_i values and four K_d values.

7.2 Discussion

For moderate K_i (0.05), the derivative term limits overshoot and helps achieve stable convergence. Large K_d values can extend the settling time or create erratic damping. At $K_i = 1.0$, the aggressive integral action drives continuous oscillations despite adding K_d. Thus, balancing K_i and K_d is key: a lower K_i makes K_d more effective at damping oscillations, whereas a high K_i can overwhelm derivative benefits and prevent fine convergence. Even a small K_d helps reduce the initial overshoot but cannot fully overcome an overly strong integral term.

8 Part 6: Heat Capacity

From the results obtained, we can determine the specific heat capacity c, which represents the amount of heat energy required to increase the temperature of a substance by a certain amount. This can be calculated using the equation $Q = mc\Delta T$, where Q is the heat energy, m is the mass, c is the specific heat capacity, and ΔT is the temperature change [2]. The maximum power that can be supplied to the aluminum rod is given by $P_{\max} = V^2 R$, where $V = 5.00 \pm 0.01\text{V}$ is the voltage we applied and $R = 3.6 \pm 0.1\Omega$ is the resistance of the heater cartridge. Consequently, we can calculate $Q = P \times t$, where $P_{applied}$ is the power applied and τ is the time constant. The resulting values are presented in Table (4).

Parameter	Value
Mass of the Aluminum (m)	0.032 ± 0.001 kg
Heat energy (Q)	597.3 ± 17.2 J
Time constant(τ)	674.71 ± 0.01 s
Temperature change (ΔT)	16.7 ± 0.1°C
Estimated heat capacity (C)	35 ± 1 J/K
Literature heat capacity (C)	28.67 J/K

Table 4: Measured and calculated values needed to calculate heat capacity [3].

The calculated heat capacity is larger than the literature value. This is presumably because the aluminum is not insulated well enough.

9 Conclusions

In this project, we implemented and compared open-loop, on/off, proportional (P), proportional-integral (PI), and proportional-integral-derivative (PID) control strategies to regulate the temperature of an aluminum rod. The open-loop tests revealed large time constants (674.71,s heating and 718.69 s cooling) caused by heat-transfer losses and the rod's thermal inertia. On/off control demonstrated easy implementation but produced oscillations around the set-point, which could be widened or narrowed by adjusting hysteresis. Proportional control reduced overshoot but could not eliminate steady-state error; tightening the proportional band improved accuracy at the risk of inducing oscillations. Adding integral action (PI) allowed the system to drive the temperature error closer to zero but introduced risks of overshoot or instability when the integral gain was too high. Incorporating a derivative term (PID) helped limit overshoot and improve settling, particularly at moderate integral gains. Lastly, we estimated the heat capacity of the aluminum rod to be around 35 ± 1 J/K, which exceeded the literature value owing to heat losses and the effective thermal mass. Overall, our results emphasize the importance of properly tuning each control term to handle thermal dynamics and ensure stable, accurate control.

References

[1] R. Woolf, "Pid tuning via classical methods," 2025, accessed: March 16, 2025. [Online]. Available: https://eng.libretexts.org/Bookshelves/Industrial_and_Systems_Engineering/Chemical_Process_Dynamics_and_Controls_%28Woolf%29/09%3A_Proportional-Integral-Derivative_%28PID%29_Control/9.03%3A_PID_Tuning_via_Classical_Methods 2

[2] LibreTexts, "Chapter 3.12: Energy and heat capacity calculations," 2025, accessed: March 16, 2025. [Online]. Available: https://chem.libretexts.org/Bookshelves/Introductory_Chemistry/Introductory_Chemistry_%28LibreTexts%29/03%3A_Matter_and_Energy/3.12%3A_Energy_and_Heat_Capacity_Calculations 9

[3] ASM International, "Asm material data sheet for 6061-t6 aluminum alloy," 2025, accessed: March 16, 2025. [Online]. Available: https://asm.matweb.com/search/specificmaterial.asp?bassnum=ma6061t6 10